Clinical Cancer Research

Extracellular HMGA1 Promotes Tumor Invasion and Metastasis in Triple-Negative Breast Cancer

Olga Méndez[1], Vicente Peg[2], Cándida Salvans[1], Mireia Pujals[1], Yolanda Fernández[3], Ibane Abasolo[3], José Pérez[4], Ana Matres[1], Marta Valeri[5], Josep Gregori[1], Laura Villarreal[1], Simó Schwartz Jr[3], Santiago Ramon y Cajal[2], Josep Tabernero[4,6], Javier Cortés[4], Joaquín Arribas[1,6,7], and Josep Villanueva[1,6]

Abstract

Purpose: The study of the cancer secretome suggests that a fraction of the intracellular proteome could play unanticipated roles in the extracellular space during tumorigenesis. A project aimed at investigating the invasive secretome led us to study the alternative extracellular function of the nuclear protein high mobility group A1 (HMGA1) in breast cancer invasion and metastasis.

Experimental Design: Antibodies against HMGA1 were tested in signaling, adhesion, migration, invasion, and metastasis assays using breast cancer cell lines and xenograft models. Fluorescence microscopy was used to determine the subcellular localization of HMGA1 in cell lines, xenograft, and patient-derived xenograft models. A cohort of triple-negative breast cancer (TNBC) patients was used to study the correlation between subcellular localization of HMGA1 and the incidence of metastasis.

Results: Our data show that treatment of invasive cells with HMGA1-blocking antibodies in the extracellular space impairs their migration and invasion abilities. We also prove that extracellular HMGA1 (eHMGA1) becomes a ligand for the Advanced glycosylation end product-specific receptor (RAGE), inducing pERK signaling and increasing migration and invasion. Using the cytoplasmic localization of HMGA1 as a surrogate marker of secretion, we showed that eHMGA1 correlates with the incidence of metastasis in a cohort of TNBC patients. Furthermore, we show that HMGA1 is enriched in the cytoplasm of tumor cells at the invasive front of primary tumors and in metastatic lesions in xenograft models.

Conclusions: Our results strongly suggest that eHMGA1 could become a novel drug target in metastatic TNBC and a biomarker predicting the onset of distant metastasis. *Clin Cancer Res; 24(24); 6367–82. ©2018 AACR.*

Introduction

Triple-negative breast cancer (TNBC) tumors represent about 15% of breast cancer cases. These tumors are usually defined by expression of basal cytokeratins and EGFR, and the lack of estrogen receptor (ER), progesterone receptor (PR), and HER2 expression (1). TNBC tumors are usually refractory to endocrine and anti-HER2 therapies, and the standard treatment is limited to generic adjuvant chemotherapy and radiotherapy (2). Furthermore, TNBC tends to be particularly aggressive and has a higher metastasis incidence than other breast cancer subtypes. Because TNBC presents a small percentage of somatic mutations, DNA sequencing approaches are not likely to provide new actionable drug targets. Therefore, new methodological approaches might be necessary to combat this subtype of breast cancer.

A big portion of the proteome involved in tumor invasion and metastatic spread such as growth factors, proteases, and cytokines performs its relevant function in the extracellular space (3). We therefore think that by profiling the fraction of the proteome that is being secreted by tumor cells, the so-called cancer secretome can shed new light over critical aspects of cancer progression in TNBC (4–6). Our lab has focused methodologically on the characterization of the cancer secretome by quantitative proteomics (6, 7). First, we developed an optimized protocol to generate cell line secretomes that were not biased by cell death and serum contamination (7). When characterizing the cancer secretome using our optimized methodology, we realized that a large portion of the proteins in the secretome profiles have no signal peptide, and hence they are not secreted through the classical ER-Golgi secretory pathway. Some of these unconventionally secreted proteins have a well-defined intracellular function (6). We have previously shown that the unconventional secretion of the EGFR correlates with the response of colorectal cancer patients to the therapeutic antibody cetuximab (8). Agreeing with our observations, proteins classically located intracellularly such as HSP90, tRNA synthetases, and HMGB1 have recently been identified in the

[1]Vall d'Hebron Institute of Oncology (VHIO), Barcelona, Spain. [2]Pathology Department, Institut de Recerca Hospital Vall d'Hebron, Barcelona, Spain. [3]CIBBIM-Nanomedicine, Vall d'Hebron Institut de Recerca (VHIR), Networking Research Center on Bioengineering, Biomaterials and Nanomedicine (CIBER-BBN), Barcelona, Spain. [4]Department of Medical Oncology, Vall d'Hebron University Hospital, Barcelona, Spain. [5]Vall d'Hebron Institut de Recerca (VHIR), Barcelona, Spain. [6]CIBERONC, Madrid, Spain. [7]Institució Catalana de Recerca i Estudis Avançats (ICREA), Barcelona, Spain.

Note: Supplementary data for this article are available at Clinical Cancer Research Online (http://clincancerres.aacrjournals.org/).

Corresponding Author: Josep Villanueva, Vall d'Hebron Institute of Oncology (VHIO), CENTRE CELLEX, C/Natzaret, 115-117, Barcelona 08035, Spain. Phone: 34 93 2543450; E-mail: jvillanueva@vhio.net

doi: 10.1158/1078-0432.CCR-18-0517

Translational Relevance

Triple-negative breast cancer (TNBC) tends to be aggressive and has a higher incidence of metastasis than other breast cancer subtypes. The standard treatment for TNBC tumors is limited to generic adjuvant chemotherapy and radiotherapy. Our studies on the breast cancer–invasive secretome suggested that a fraction of the intracellular proteome could play an unanticipated role in the extracellular space during tumorigenesis. Here, we show that the nuclear protein high mobility group A1 (HMGA1) is oversecreted in a regulated fashion in TNBC cells. Our data show that treatment of invasive TNBC cells with HMGA1 antibodies in the extracellular space impairs their migration and invasion abilities. We also prove that the subcellular localization of HMGA1 correlates with the incidence of metastasis in a cohort of TNBC patients. Our data suggest that eHMGA1 could become a novel drug target in metastatic TNBC and a biomarker predicting the onset of distant metastasis.

extracellular space performing alternative functions related to cancer (9–11). Unconventional secretion refers to a series of ER-Golgi–independent routes to secrete proteins to the extracellular space. Usually, these proteins reach the extracellular space as cargo of vesicles such as exosomes and plasma membrane–derived microvesicles, as well as directly traversing the plasma membrane using protein transporters or specific phospholipids (12, 13). During the last few years, it has become evident that intracellular proteins compose a large fraction of the secretome, although the function of the vast majority of these unconventionally secreted proteins is unknown.

A project undertaken in our lab, and aimed at investigating the TNBC-invasive secretome, identified several proteins nonclassically secreted related to an invasive phenotype that could be relevant for cancer research (7). Among them, we chose to study the alternative extracellular function of high mobility group A1 (HMGA1) in tumor invasion and metastasis. HMGA1 is a nuclear protein that binds to the minor groove of AT-rich DNA strands and controls the transcriptional activity of several genes (14). HMGA1 is normally expressed at high levels during embryonic development and at low or absent levels in adult normal tissues (15). Despite mutations, amplification, or rearrangements of the HMGA1 gene have not been described in solid tumors, HMGA1 overexpression is often observed in advanced cancers. Besides, HMGA1 overexpression frequently correlates with the presence of metastasis and reduced patient survival (16–18). Most of the mechanisms proposed for the HMGA1 role in tumorigenesis are based on transcriptional regulation of genes that have a key role in the control of cell proliferation and DNA repair (16). However, there is no clear mechanistic explanation reported for the correlation of HMGA1 overexpression and the observed increased incidence of metastasis.

In this study, we demonstrate that despite HMGA1 is a nuclear protein with a defined transcriptional activity, it is also secreted in invasive TNBC cells. We demonstrate that HMGA1 is unconventionally secreted, and its secretion is mediated by Casein Kinase 2 (CK2). We also show performing either *in vitro* or *in vivo* assays that extracellular HMGA1 (eHMGA1) mediates migration, invasion, and metastasis. Using blocking antibodies against HMGA1, we are able to impair invasion in TNBC tumor cells *in vitro* and decrease the incidence of distant metastasis in *in vivo* assays. The mechanistic studies shown in this work prove that HMGA1 is secreted in a regulated fashion and, once in the extracellular space, becomes a ligand for Advanced glycosylation end product-specific receptor (RAGE), a plasma membrane receptor, which signals through pERK, and it is linked to adhesion, migration, invasion, and metastasis. Furthermore, we established a correlation between the secretion of HMGA1 and its change of subcellular localization in invasive cells. We found that a change from nuclear to cytoplasmic localization of HMGA1 predicts the aggressiveness of TNBC primary tumors. Interestingly, our work shows that it is the secreted form of HMGA1 that explains its role in tumor invasion and metastasis. These results conceptually change the view on HMGA1's role in tumorigenesis and highlight the relevance of unconventional protein secretion in cancer diagnostics and therapeutics.

Materials and Methods

Cell culture and treatments

All breast cancer cell lines were obtained from the ATCC and cultured in 5% CO_2 and 95% humidified atmosphere air at 37°C. MDA-MB-231, MCF-7, and Hs578T cell lines were cultured in DMEM (DMEM/F12; Invitrogen), and BT549 cells were cultured in RPMI (Invitrogen). All cell lines were supplemented with 10% FBS (Invitrogen) and 2 mmol/L L-Glutamine (Invitrogen). The cell lines were authenticated by short tamdem repeat profiling (IdentiCell, Aarthus University Hospital). All cell lines were tested by PCR, to ensure they were Mycoplasma negative before being used for any experiment. In order to enhance the invasive phenotype of MDA-MB-231 cells, a highly invasive subline (MDA231i) was derived by five consecutive rounds of *in vitro* selection using Boyden chambers coated with matrigel. MDA231i cells were transfected using X-Treme-Gene (Roche) with the plasmid pGL4 expressing the firefly luciferase 2 (*Photinus pyralis*) gene (kindly provided by Dr. Abasolo, CIBBIM-Nanomedicine, VHIR). MDA231i cells were also transfected with the plasmid pIRES-HMGA1 (Addgene) and with pcDNA-HMGA1-C-6His-tag (Genscript). Transfectants were selected with G418 and puromycin when suitable.

MEK inhibitor (AZD6244; Selleckchem) was used at 10 μmol/L. When needed, MDA231i/shHMGA1 cells were treated with 1 μg of rHMGA1 and 50 ng/mL of recombinant human RAGE (R&D systems). MDA231i cells were treated with 1 μg/mL of HMGA1-Ab (Santa Cruz Biotechnology). rHMGA1 protein expression and purification was performed by the ICTS "NANBIOSIS," more specifically by the Protein Production Platform of CIBER in Bioengineering, Biomaterials and Nanomedicine (CIBER-BBN)/IBB, at the UAB (Universitat Autònoma de Barcelona) (http://www.ciber-bbn.es/en/programas/89-plataforma-de-produccion-de-proteinas-ppp). Briefly, rHMGA1 containing a HIS-tag at the C-terminal end was produced in *Escherichia coli* and purified by Ni-NTA affinity chromatography.

Secretome sample preparation and treatments

Secretomes were prepared as previously described (7). Briefly, 4×10^6 cells in exponential phase were seeded in 150 cc tissue culture plates and allowed to grow for 48 hours. After that, media were aspirated, and cells were washed 5 times, 2 times

with PBS and the last 3 with serum-free media. After that, cells were maintained for the indicated time in the presence of serum-free media before collecting the conditioned media (secretome). The conditioned media were spun down at 200 g for 5 minutes, and the supernatants were collected and filtered through a Millex-GP 0.22 μm pore syringe-driven filter (Millipore). Then, secretomes were concentrated using a 10,000 MWCO Millipore Amicon Ultra (Millipore). Protein concentration was determined with a Pierce BCA protein assay kit (Thermo Scientific).

The CK2 inhibitors CX4945 (Santa Cruz Biotechnology) and TBB (Santa Cruz Biotechnology) were used at 5 μmol/L and 0.05 mmol/L, respectively. When suitable, secretomes were done in the presence of Brefeldin A (Sigma-Aldrich; 20 ng/mL) and treated with 30 μg/mL elastase (Sigma-Aldrich) and 1% triton (Sigma-Aldrich).

Lentivirus production and infection of breast cancer cells

Three different shRNA sequences directed against HMGA1 were purchased from Open Biosystems (GE Healthcare) and used to knockdown HMGA1 expression in MDA231i breast cancer cell lines. Recombinant lentiviruses were produced by cotransfecting HEK 293T cells with the lentivirus expression vector (pGIPZ puro) and packaging plasmids (Δ8.9 and vsv-g) using X-TremeGene as a transfection reagent. Infectious lentiviruses were collected at 24, 48, and 72 hours after transfection and the pooled supernatants centrifuged to remove cell debris and filtered through a 0.45 μm filtration unit. MDA231i cells were infected, and stable transfectants were selected in puromycin. The sequence selected for further analysis (shHMGA1) was based on both downregulation of HMGA1 expression based on WB analysis and its ability to reduced invasion as assessed by Boyden chambers. Lentivirus-expressing shRNA against CK2 and RAGE was done following the same protocol.

These are the shRNA sequences used to perform the experiments: shHMGA1 (ctccctctctggtttccta; tgcagttacttgaataaaa; ccgaccaaagggaagcaaa), shCK2 (accagctggttcgaaaatt; ggccctatctgtctcctga; agagtttacacagatgtta), and shRAGE (ccaggcaatgaacaggaat).

Boyden chamber invasion assay

BD Biocoat chambers (Corning Life Sciences) with 8-μm pore size polystyrene filter inserts for 24-well plates were coated with matrigel (BD Biosciences) and used according to the manufacturer's instructions and as described (19). Briefly, cells were seeded onto the upper compartment of each chamber in 300 μL of DMEM without FBS and placed into wells containing 750 μL of complete medium in the lower chamber. After 24 hours, the inserts were fixed and stained, and the number of invading cells was counted as described (19). Three independent experiments, done in triplicate, were performed. Images were quantified using Image J software (NIH, Bethesda, MD).

Wound-healing assay

Cells were grown to confluence in 6-well plates. Cell monolayers were scratched with a sterile yellow pipette tip and washed with PBS to remove detached cells. Fresh media with the appropriate treatment were added when needed. Phase contrast images were taken with an Olympus FSX100 microscope immediately and at the indicated time points. The wound area was measure using Image J software.

MTT proliferation assay

Cells (5×10^3) were seeded into 96-well plates. Cell growth was determined every 24 hours by using the Thiazolyl Blue Tetrazolium Bromide (MTT, Sigma-Aldrich) metabolic assay. Four replicates per condition were assayed.

Western blot and coimmunoprecipitation

Cells were seeded in complete growth medium and allowed to grow at the specified times and conditions. Total protein extraction was done using NP-40 lysis buffer. When needed, nuclear and cytoplasmic proteins were extracted according to manufacturer's instructions (NE-PER Nuclear and Cytoplasmic Extraction Reagents; Thermo Scientific). Protein quantitation and electrophoresis were performed as described elsewhere. Western blot (WB) analysis was performed with the following primary antibodies: rabbit anti-HMGA1 (sc-8982 and sc-393213; Santa Cruz Biotechnology), mouse anti–alpha-tubulin (clone B-5-1-2, #T9026; Sigma-Aldrich) used at 1:10,000, rabbit anti-pERK (Thr202/Tyr204, #9101S), rabbit anti-ERK (#9102S), rabbit anti-pAKT (Ser473, #9271), rabbit anti-AKT (#9272), rabbit anti-pSrc (Tyr416, #2101; all of them from Cell Signaling Technology), rabbit anti-pSmad2 (Ser465/467; AB3849; Chemicon International), mouse anti-fibronectin (#610078; BD Biosciences), mouse anti-CK2α (#2656; Cell Signaling Technology), rabbit anti-RAGE (Ab3611; Abcam), and mouse anti-TSG101 (Ab83; Abcam) used at 1:500. Horseradish peroxidase–conjugated secondary antibodies were sheep anti-mouse (NA931) and donkey anti-rabbit (NA934) IgG (GE Healthcare). All antibodies, at least otherwise stated, were used at 1:1,000. Immunodetection was followed by visualization and densitometry using Image J software.

Coimmunoprecipitation experiments were done using pure-proteome nickel magnetic beads (Millipore) and Dynabeads Proteins A (Invitrogen) following the manufacturer's instructions.

Surface plasmon resonance

Surface plasmon resonance (SPR) analyses were performed at 25°C on a Biacore T200 (GE Healthcare BioSciences AB). Note that 10 μg/mL of recombinant Rage (#1145-RG; R&D systems) was diluted in 10 mmol/L acetate buffer, pH 5.5, and immobilized on a CM5 chip by amine coupling. Briefly, the surface was activated with a mixture of 1:1 mixture of 0.1 mol/L NHS (N-hydroxysuccinimide) and 0.1 mol/L EDC (3-(N,N-dimethylamino) propyl-N-ethylcarbodiimide) at a flow rate of 5 μL/min, followed by the injection of ligand or buffer for the active or reference channel respectively. Ethanolamine solution was injected in both channels in order to block the remaining reactive groups of the surface. HMGA1 (0, 0.312, 0.625, 1.25, 2.5, 5, and 10 μgr/mL) was prepared in running buffer, HBS-P (phosphate buffer saline 0.005% P20) 2% Glycerol, and was injected in both channels at 20 μL/min flow for 90 seconds and dissociation time of 200 seconds. The complexes formed were regenerated with NaOH 50 mmol/L. Relative response was expressed in resonance units, and sensorgrams were double zero-reference (reference channel and blank subtraction).

Adhesion assay

Twenty-four–well plates were coated overnight (O/N) at 4°C with 10 μg/mL of fibronectin or laminin (both from Santa Cruz Biotechnology). Afterward, plates were maintained at 37°C for 1 hour. Coating was washed with PBS and blocked with DMEM

for 30 minutes at 37°C before seeding the cells. Briefly, 100,000 cells (MDA231i, MDA231i/shHMGA1) or 50,000 cells (BT549) were seeded in each well. After 1 hour, cells were washed and fixed. Adherent cells were stained with crystal violet. After solubilization with acetic acid 10% plates were read at 560 nm. When suitable, cells were pretreated beforehand with HMGA1 Ab or rHMGA1 as previously described.

Immunofluorescence and confocal microscopy of breast cancer cells and tissue sections

Cells were seeded on collagen-coated glass coverslips. After growing them for the appropriate time, cells were fixed with paraformaldehyde 4% for 30 minutes and permeabilized with 0.2% triton for 15 minutes.

Immunostaining of human and mice tumor samples was performed on paraffin-embedded tissues. Tissue blocks were sectioned, mounted on microscope slides, and heated at 56°C O/N. Paraffin was removed with xylene, and tissues were serially rehydrated through descending ethanol concentrations to water. Sections were stained with hematoxylin and eosin (H&E) to assess cellular morphology. For immunofluorescence (IF), antigen retrieval was performed by boiling the samples in EDTA (Calbiochem) buffer 994,1 μmol/L (pH 8), using a microwave oven. Slides were then washed twice in PBS and once in PBS-1% Tween-20 (Sigma-Aldrich) for 15 minutes. Unspecific binding sites, for both cells and tissues, were blocked by incubating with 3% BSA (Sigma-Aldrich) for 1 hour. Primary antibodies were prepared in 3% BSA and incubated O/N at 4°C: rabbit anti-HMGA1 (Santa Cruz Biotechnology) was used at 1:100 for cells and 1:200 for tissues, and mouse anti-Cytokeratin (clones AE1/AE3; Dako) was used at 1:100 for tissue samples. Primary antibody incubations were followed by PBS washes and incubation for 1 hour at room temperature with the appropriate secondary antibody (goat anti-mouse and goat anti-rabbit) conjugated to Alexa Fluor 555 and Alexa Fluor 488 (Invitrogen). Phalloidin (Phalloidin–Tetramethylrhodamine B isothiocyanate; Sigma-Aldrich) was used to stain actin cytoskeleton of cells. Nuclei were stained with Hoechst 33342 (5 μg/mL; Sigma-Aldrich). An Olympus FluoView FV1000 Confocal Microscope was used to visualize fluorescence and acquire images from five representative fields of each sample. HMGA1 nuclear and cytoplasmic expression was measured in confocal images using Image J software.

In vivo tumorigenic and metastatic assays

Female-immunodeficient NOD-SCID (NOD.CB17-Prkdcscid/J) mice (Charles River Laboratories) were kept in pathogen-free conditions and used at 7 weeks of age. Animal care was handled in accordance with the Guide for the Care and Use of Laboratory Animals of the Vall d'Hebron University Hospital Animal Facility, and the Animal Experimentation Ethical Committee at the institution-approved experimental procedures. All the *in vivo* studies were performed by the ICTS "NANBIOSIS" at the CIBER-BBN's *In Vivo* Experimental Platform of the Functional Validation & Preclinical Research (FVPR) area.

Different variants of MDA231i cells (shControl, shHMGA1, IgG pretreatment, and HMGA1-Ab pretreatment, 5×10^6) expressing the luciferase gene were suspended in 200 μL of PBS with matrigel (1:1; BD Bioscience) and implanted into the right abdominal mammary fat pad (i.m.f.p.). Tumor growth was monitored twice a week by conventional caliper measurements ($D \times d^2/2$, where D is the major diameter and d the minor diameter). When tumor volumes reached 300 to 400 mm^3, primary tumors were excised and weighted, and lungs and lymph nodes tissues were examined for the presence of metastatic *foci* by *ex vivo* bioluminescence imaging (BLI) and histopathology. BLI was performed using an IVIS Spectrum Imaging System (PerkinElmer Life Science), and images were acquired and analyzed using the Living Image 4.3 software (PerkinElmer). To do so, mice were injected intraperitoneally with 150 mg/kg of D-luciferin (Promega) prior to euthanasia. Immediately postmortem, organs of interest were washed with PBS and placed individually into separate wells with 300 μg/mL of D-luciferin and imaged. Then, tissues were washed with PBS, fixed in 4% formaldehyde solution, and embedded in paraffin for H&E staining.

Tumor interstitial fluid

Tumor interstitial fluids (TIF) were generated right after tumor excision from mice. Tumor tissue was put immediately on ice and kept in cell culture media without serum. Tumor was mince into pieces of approximate 2 mm and incubated with 4 mL of PBS during 1 hour at 37°C. After that, TIF was collected, spun at maximum speed, filtered with 0.2 μm, and kept at −80°C until needed. Protein concentration was determined with a Pierce BCA protein assay kit (Thermo Scientific).

Patient samples

All clinical samples were obtained from Vall d'Hebron University Hospital (Barcelona, Spain). The study was approved by the hospital ethical committee, including a waiver of consent for the use of archival material for research.

Statistical analysis

Statistical significance was determined using GraphPad Prism Software.

Results

HMGA1 is overexpressed and secreted in a regulated fashion in breast cancer–invasive cells

To understand the role of unconventional secretion in the context of tumor invasion in TNBC cells, we reanalyzed the SILAC-based secretome data of a comparative analysis performed in our lab between a TNBC-invasive cell line (MDA-MB-231) and a noninvasive breast cancer cell line (MCF-7; ref. 7). Secretomes derived from the two cell lines had been profiled by liquid chromatography mass spectrometry, and the data were analyzed by differential expression statistics (7, 20). We took theoretically nuclear proteins that were observed in the secretome dataset and checked their expression levels in human breast tissue (7). We considered that the translocation from the nucleus to the cytoplasm in the tissue staining could be a surrogate of the protein secretion observed in secretomes. Therefore, nuclear proteins with cytoplasmic staining were taken as potential candidate proteins unconventionally secreted. Among the different proteins found that fit these criteria, we decided to further study HMGA1. On the one hand, this protein showed a clear cytoplasmic staining in breast tumors in the Human Protein Atlas database (Fig. 1A). On the other hand, a close relative of HMGA1, HMGB1, is already known to be unconventionally secreted and linked to cancer (21–23).

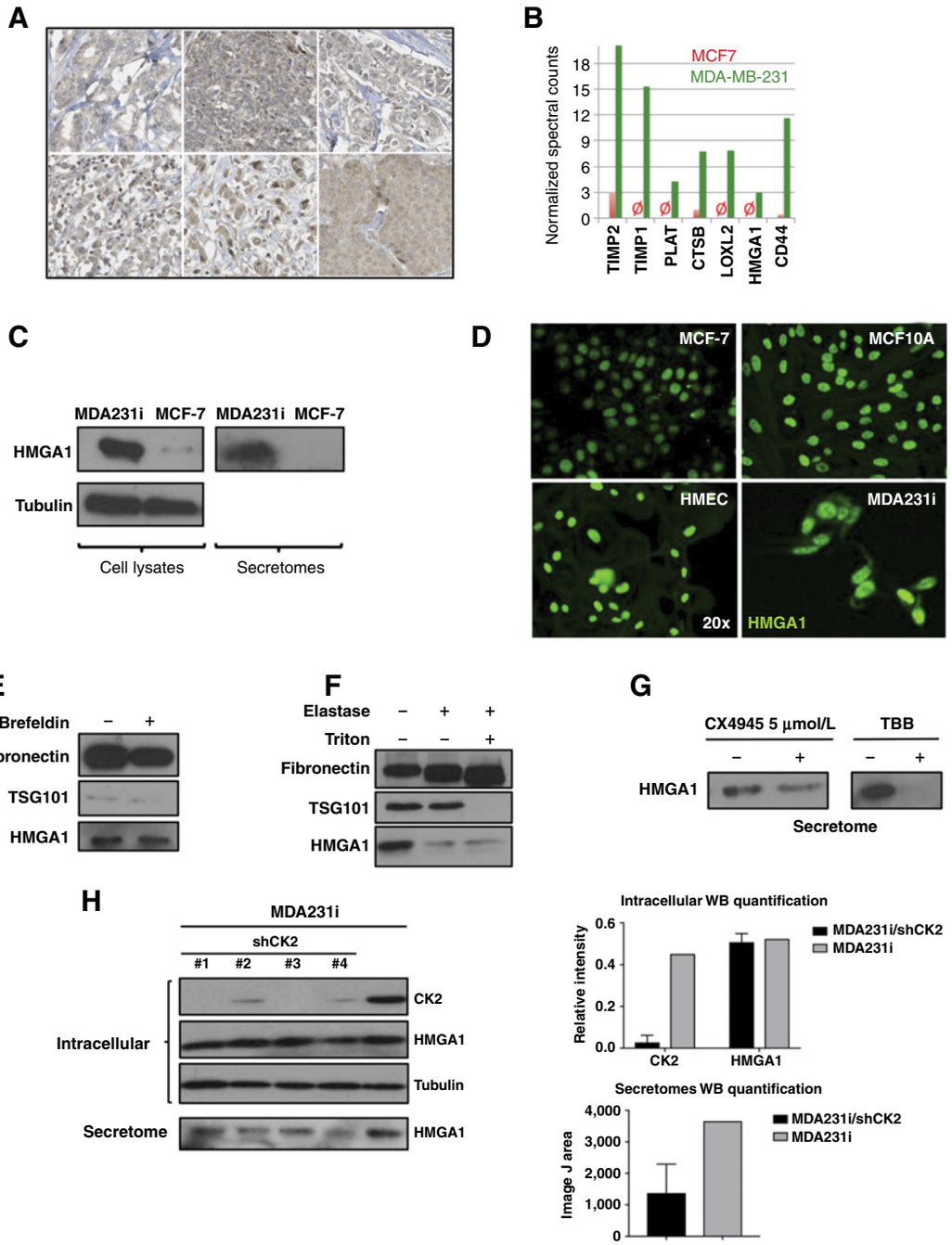

Figure 1.

HMGA1 is overexpressed and secreted in a regulated fashion in TNBC-invasive cells. **A,** IHC analysis from the Protein Atlas database of HMGA1 in different breast tumors shows a clear cytoplasmic staining. **B,** Graph representing the fold changes of a group of selected proteins differentially secreted between MDA231i and MCF-7 cells. Among them, we chose to further validate HMGA1. **C,** WB showing HMGA1 expression (cell lysate and secretome) in MDA231i and MCF-7 cells. Tubulin was used as loading control when suitable. **D,** IF (20X) showing HMGA1 expression (in green) in MCF-7, MCF10A, HMEC, and MDA231i cells. **E,** WB of MDA231i cells secretomes done in the presence or absence of brefeldin (BFA), an inhibitor of ER to Golgi transport. Fibronectin, a classically secreted protein, TSG101, an exosomal protein, and HMGA1 levels are shown. HMGA1 secretion is not affected by BFA treatment. **F,** WB of MDA231i cells secretomes treated with elastase (serine protease), triton X-100 (nonionic surfactant that can permeabilize vesicles), or the combination of both. Fibronectin, TSG101, and HMGA1 levels are shown. Elastase alone or in combination with triton X-100 reduces HMGA1 levels. **G,** WB showing HMGA1 expression levels in MDA231i cells after the pharmacologic inhibition of CK2, by treatment with CX4945 and TBB, both selective inhibitors of CK2. The two treatments reduce the secretion of HMGA1. **H** (Left plot), WB of MDA231i cells expressing shCK2 sequences and control cells. Levels of CK2 (intracellular) and HMGA1 (intracellular and secretome) are shown. Tubulin was used as loading control when suitable. Right plot, Graphs showing intracellular WB ratios of CK2 and HMGA1, as well as the quantification of the secretion of HMGA1 in MDA231/shCK2 cells versus MDA231i cells. In both cases, the data obtained from the four different shCK2 sequences were average.

Furthermore, this protein had a clear interest in cancer research because it has been related to tumor aggressiveness and incidence of metastasis (24–27). We found that HMGA1 was oversecreted in invasive cells (MDA-MB-231) with respect of noninvasive cells (MCF-7), along with other proteins already related to invasion (CD44, TIMP2, PLAU, and LOXL2; Fig. 1B; ref. 7). Moreover, despite the fact that HMGA1 it is rarely mutated or amplified in tumors, its overexpression is often observed in the basal-like subtype (28), to which MD-MB-231 cells relate (Supplementary Fig. S1).

To enhance the invasive phenotype of MDA-MB-231 cells, a highly invasive subline (MDA231i) was derived and used for all the experiments in this work (see Materials and Methods). In order to confirm the previous proteomic experiments, secretomes and cell lysates of MDA231i and MCF-7 cells were analyzed by WB (Fig. 1C). Results showed both a higher intracellular expression and secretion of HMGA1 in the invasive cell line compared with the noninvasive cells. To further characterize HMGA1 levels in breast cancer cells, we analyzed its subcellular localization in breast epithelial cells with different tumorigenic potential. Although HMGA1 was weakly expressed in the nucleus of nontransformed human mammary epithelial cells (HMEC), its expression was higher, but still only nuclear, in nontumorigenic (MCF10A cells) and tumorigenic though weakly invasive breast tumor cells such as MCF-7 (Fig. 1D). However, in highly invasive cells (MDA231i), HMGA1 showed a high expression in the nucleus but also in the cytoplasm (Fig. 1D), which is consistent with the observed oversecretion (Supplementary Fig. S2).

Before characterizing the role and the possible implications of eHMGA1 in tumor invasion, we first wanted to know how HMGA1 is being secreted. Initially, we confirmed that HMGA1 is not secreted through the classically ER-Golgi secretory pathway. Our data show that secretomes derived from MDA231i cells in the presence of brefeldin A, a known inhibitor of classical secretion, show a reduction in the secretion level of the classically secreted protein fibronectin, whereas do not affect the levels of either TSG101, a known marker of exosomes, or HMGA1 (Fig. 1E). Next, we studied whether HMGA1 is secreted through extracellular vesicles such as exosomes or plasma membrane–derived microvesicles. The MDA231i secretomes were treated with elastase (a serine protease), triton X-100 (a nonionic detergent), or the combination of both. Our data show that fibronectin is degraded in the presence of either elastase or triton/elastase, whereas TSG101 is only degraded when secretomes are treated with detergent. The results also show that HMGA1 is not protected by vesicles, although it is nonclassically secreted (Fig. 1F). To further support that HMGA1 is secreted from living tumor cells, we wanted to show that its secretion could be regulated by testing the possible implication of CK2. Previous work has shown that CK2 is involved in the unconventional secretion of different proteins (29–31). Because the C-terminal tail of HMGA1 is known to be phosphorylated by CK2 and this region has previously been related to aggressiveness in cancer (32), we decided to study its possible role in HMGA1 secretion. Our data showed that both the pharmacologic inhibition of CK2 (Fig. 1G) and the ablation of its gene expression using short hairpins severely reduced the secretion of HMGA1 in MDA231i cells (Fig. 1H), whereas do not affect significantly its intracellular expression, proving that CK2 is involved in the secretion of HMGA1.

Secreted HMGA1 mediates an invasive phenotype in breast cancer cells

Once we had determined that HMGA1 is being secreted in a regulated fashion in TNBC cells, we wanted to test whether it is required for the invasive phenotype of these cells. We stably knocked it down (MDA231i/shHMGA1) and overexpressed it (MDA231i/HMGA1) in MDA231i cells. The ablation of HMGA1 expression resulted in a 3-fold decrease in its secretion, whereas its overexpression resulted in a 3-fold oversecretion compared with the parental MDA231i cells (Fig. 2A). Although cell proliferation was not affected by the perturbation of HMGA1 expression levels (Fig. 2B), the results showed that shHMGA1 cells had diminished migration and invasion capabilities with respect to MDA231i cells (Fig. 2C and F). Conversely, MDA231i/HMGA1 cells migrated faster than MDA231i cells (Fig. 2C). Nonetheless, in order to truly evidence the role of the extracellular form of HMGA1 as a key factor in the invasiveness of breast cancer, the migration and invasion of MDA231i cells were evaluated in the presence of an Ab against HMGA1, showing that blocking eHMGA1 reduces both migration and invasion while does not affect proliferation (Fig. 2D and E; Supplementary Figs. S3 and S4). Furthermore, as an additional control that the HMGA1 Ab targets the extracellular form of HMGA1, we have tested that the Ab is not internalized by MDA231i cells (Supplementary Fig. S5). Two different Abs against HMGA1 equally blocked tumor migration, whereas an unspecific IgG did not (Supplementary Fig. S3B). Blocking eHMGA1 in other highly invasive TNBC cells (BT549 and Hs578T) also diminished their migration and invasion abilities (Fig. 2E; Supplementary Fig. S6). We also established that an Ab against HMGA1 could block the invasion of shHMGA1 cells that had previously recovered the invasive phenotype by treatment with the conditioned medium (CM) of MDA231i cells (Fig. 2F). We also showed that the CM of MDA231i cells increased the invasive phenotype of MCF-7, but this effect was largely blocked when an Ab against HMGA1 was present in the media (Supplementary Fig. S7). Finally, the invasive phenotype of MDA231/shHMGA1 cells was recovered by treating them with a recombinant HMGA1 protein (rHMGA1), showing that eHMGA1 is implicated in the invasive phenotype of TNBC cells *in vitro* (Fig. 2G).

Secreted HMGA1 signals through pERK

To characterize the molecular mechanism used by eHMGA1 to mediate tumor invasion in the extracellular space, we first tested whether eHMGA1 could activate any of the usual intermediate signaling nodes involved in signal transduction events. The overexpression and the knockdown of HMGA1 in MDA231i cells showed differences in the activation of ERK1/2 signaling, whereas the activation of other nodes such as AKT and Src does not seem implicated in HMGA1-mediated invasion in MDA231i cells (Fig. 3A; Supplementary Fig. S8). In addition, we showed that rHMGA1 increases in a dose-dependent manner the activation of pERK in shHMGA1 cells (Fig. 3B), whereas an HMGA1-Ab abrogates pERK activation both in MDA231i/shHMGA1 cells treated with rHMGA1 (Fig. 3B) and in MDA231i cells (Fig. 3C). To confirm these findings, we demonstrated that rHMGA1 increased the migration of MDA231i/shHMGA1 cells and that a MEK inhibitor (AZD6244) abolished the increased migration induced by rHMGA1 (Fig. 3D). The fact that HMGA1-Ab blocks pERK activation (Fig. 3B and C) implies that it could

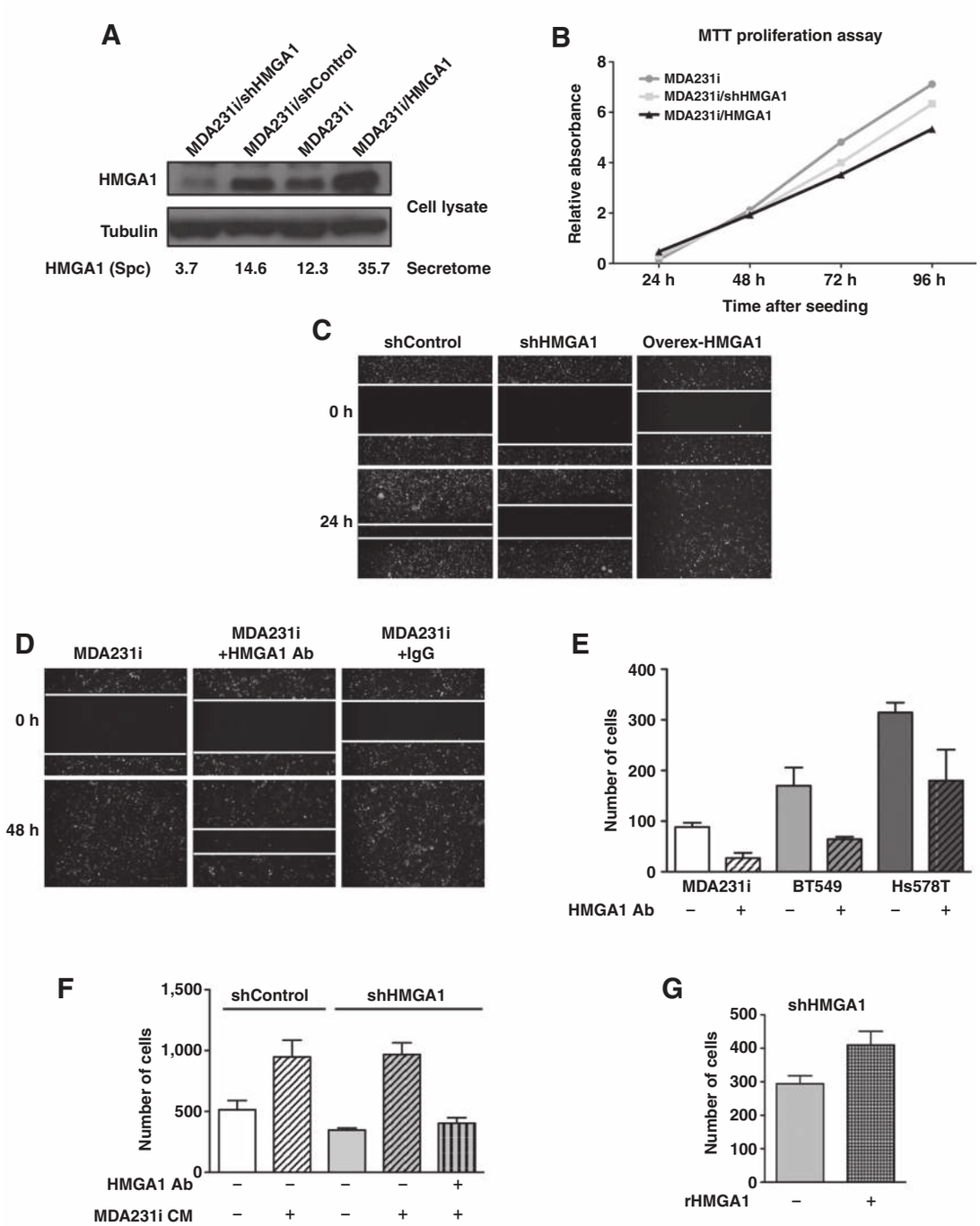

Figure 2.

Secreted HMGA1 mediates an invasive phenotype in breast cancer cells. **A,** WB showing HMGA1 expression levels in MDA231i/shHMGA1, MDA231i/shControl, MDA231i, and MDA231i/HMGA1 cells. Tubulin was used as loading control. The number of spectral counts (Spc) detected in the secretomes of the corresponding cell lines after mass spectrometry analysis is shown. **B,** Graph representing cell proliferation measured by MTT assay at 24, 48, 72, and 96 hours after seeding. Relative absorbance is represented for each time point and cell line. No significant proliferation effects are seen. **C,** Wound assay of MDA231i cells expressing different levels of HMGA1. Pictures are shown at 0 and 24 hours. White lines show the margins of the wounds. MDA231i/shHMGA1 cells migrated less as compared with control cells, whereas cells overexpressing HMGA1 (MDA231i/HMGA1) showed an increase in their migration ability. **D,** Wound assays of MDA231i cells used as control, and treated either with HMGA1-Ab or with an unspecific IgG. Pictures are shown at 0 and 48 hours. White lines show the margins of the wounds. **E,** Graph showing invasion assays results after 24 hours for MDA231i, BT549, and Hs578T cell lines treated with HMGA1-Ab (striped bars) or untreated (smooth bars). **F,** Graph showing the number of cells measured by invasion assay after 24 hours. MDA231i/shHMGA1 cells have a reduced invasion ability as compared with control cells. Treatment of the cells with CM from MDA231i increased their invasion ability, and this can be abrogated to the original levels by treatment with HMGA1-Ab. **G,** Graph showing the number of cells measured by invasion assay after 24 hours. Treatment of MDA231i/shHMGA1 cells with rHMGA1 protein rescued their invasive phenotype.

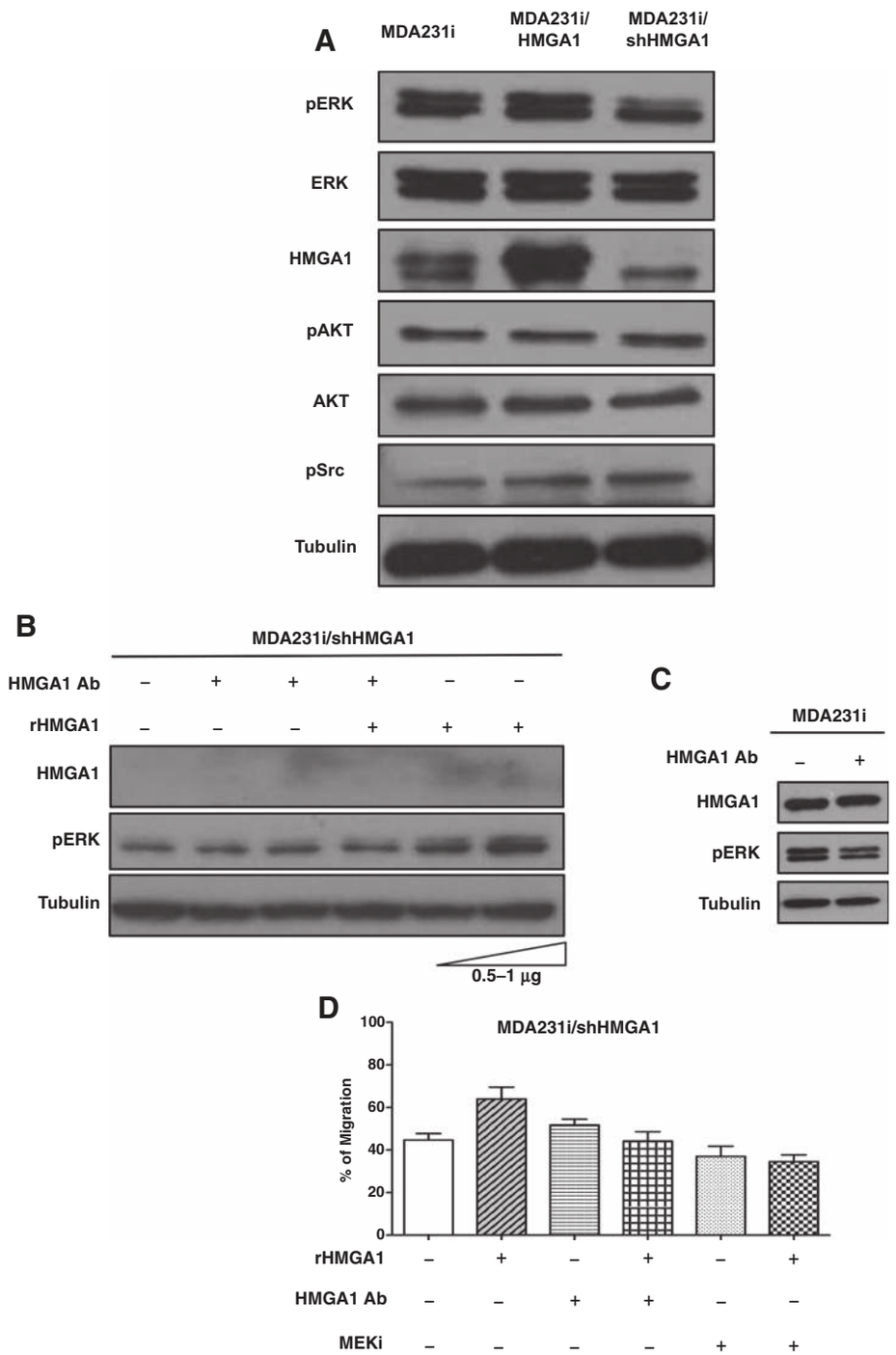

Figure 3.
Secreted HMGA1 signals through pERK. **A,** WB of MDA231i cells, and the variants overexpressing and silencing HMGA1. The expression levels of pERK, ERK, pAKT, AKT, pSrc, and HMGA1 are shown. Tubulin was used as loading control. **B,** WB of MDA231i/shHMGA1 cells treated with HMGA1-Ab, rHMGA1, or the combination. HMGA1 and pERK expression levels are shown. Tubulin was used as loading control. **C,** WB of MDA231i cells treated with or without HMGA1-Ab. The expression levels of HMGA1 and pERK are shown. Tubulin was used as loading control. Ab treatment reduces pERK levels. **D,** Graph showing the percentage of migration of MDA231i/shHMGA1 measured by wound assay. Treatment of the cells with rHMGA1 increased their migration ability, which was abrogated in the presence of HMGA1-Ab and in the presence of a MEKi.

therefore represent a possible therapeutic option against eHMGA1. Accordingly, our data show that treatment with HMGA1 Ab blocks migration of MDA231i cells (Fig. 2D).

eHMGA1 binds to RAGE inducing pERK signaling and having an impact on cell adhesion

The signaling of eHMGA1 through pERK, together with the fact that eHMGA1 is not internalized after secretion (Supplementary Fig. S9), led us to seek for a membrane receptor that could transduce its signal from the extracellular space. Among different strategies, we studied the possible implication of RAGE in the extracellular signaling of HMGA1. RAGE is the receptor for another HMGA1 family member, HMGB1, as well as for several proteins of the S100 family (33, 34). Moreover, RAGE is known to signal through pERK in TNBC and to mediate tumor cell migration (35). We first showed that

HMGA1 and RAGE bind to each other in coimmunoprecipitation experiments (Fig. 4A). Then, we show that RAGE and HMGA1 colocalize in the plasma membrane of nonpermeabilized MDA231i cells (Fig. 4B). To further confirm the interaction between RAGE and HMGA1, we performed SPR analysis using the extracellular domain of RAGE, which contains the binding site for its known ligands and our rHMGA1. The analysis of the sensorgram obtained after using 0, 0.312, 0.625, 1.25, 2.5, 5, and 10 μgr/mL of rHMGA1 over immobilized RAGE shows that there is a dose response binding of rHMGA1 to RAGE. These results indicate that HMGA1 is a direct partner of RAGE (Fig. 4C). We also showed that the soluble extracellular domain of RAGE interferes with the migratory phenotype and with the activation of pERK induced by rHMGA1 on MDA231i/shHMGA1 cells (Fig. 4D; Supplementary Fig. S10). To further prove the link between HMGA1 and RAGE, we showed that the double-knockdown (HMGA1 and RAGE) MDA231i cells are insensitive to rHMGA1, confirming that HMGA1 signals through RAGE (Fig. 4E; Supplementary Fig. S11). Next, we wanted to learn how the binding of eHMGA1 to RAGE could impact on the invasive phenotype of MDA231i cells. Because RAGE has been previously linked to cellular adhesion, we first tested whether the perturbation of eHMGA1 affects adhesion. Both MDA231i/shHMGA1 and MDA231i cells treated with HMGA1-Ab are more adherent to ECM (laminin and fibronectin) proteins than MDA231i cells (Fig. 4F). Furthermore, MDA231i/shHMGA1 treated with rHMGA1 are less adherent than MDA231i/shHMGA1 cells (Fig. 4G). In agreement with the adhesion phenotype observed in MDA231i cells with reduced levels of HMGA1, BT549 cells treated with HMGA1 Ab show as well a decreased adhesion to ECM proteins (Fig. 4H).

eHMGA1 promotes metastasis in TNBC

To validate the *in vivo* role of HMGA1 in breast cancer invasion, MDA231i/shHMGA1 and MDA231i/shControl cells were implanted orthotopically into the mammary fat pad (i.m.f.p.) of female NOD-SCID mice. The growth rates of MDA231i/shHMGA1 and MDA231i/shControl tumors were similar along time (absolute growth delay of 2 days) and not statistically significant at the end time point ($P = 0.0770$; Fig. 5A, top). However, *ex vivo* BLI and histopathology (Supplementary Fig. S12) confirmed that MDA231i/shHMGA1 reduced the incidence of distant metastasis. The global analysis of all the metastasis detected in the different organs, analyzed by *ex vivo* BLI, shows that MDA231i/shHMGA1 cells are less metastatic (P value = 0.0361; Wilcoxon matched-pairs signed rank test) than control cells (Fig. 5A, bottom; Supplementary Fig. S13). Furthermore, pERK immunostaining showed a clear reduction in pERK levels in tumors derived from MDA231i/shHMGA1 cells in comparison with tumors derived from MDA231i/shControl cells (Fig. 5B), confirming our *in vitro* results (Fig. 3A).

To further evaluate the implication of HMGA1 in metastasis and invasion, the control group of the previous *in vivo* experiment (Fig. 5A) was used to analyze the localization of HMGA1. IF of HMGA1 on the primary tumors and metastasis of these mice showed strong cytoplasmic levels consistent with an alteration in the subcellular localization of HMGA1. In addition, IF on primary tumors suggested a gradient in HMGA1's expression that increased toward the invasive front of the tumor (Fig. 5C, top; Supplementary Fig. S14). The high expression of HMGA1 at the tumor-invasive front was accompanied by a high expression in lymph nodes and distant metastasis, indicated by the presence of metastatic *foci* in the lungs (Fig. 5C, bottom; Supplementary Fig. S15). To confirm that the cytoplasmic expression of HMGA1 correlates with its secretion, we analyzed by WB the presence of HMGA1 in TIFs derived from MDA231i tumor xenografts (Fig. 5D). Results confirmed that tumor cells secreted HMGA1 and that a cytoplasmic localization of HMGA1 correlates with its secretion *in vivo*.

In vitro experiments showed that MDA231i cells treated with HMGA1 Ab lost their migratory phenotype (Fig. 2D). Considering that, we explored the influence of blocking the extracellular function of HMGA1 *in vivo* by pretreating MDA231i cells with either an HMGA1-Ab or an unspecific IgG before implanting them into mice. As previously observed when we knocked down HMGA1 *in vivo*, the growth rates of tumors derived from Ab pretreated cells (MDA231i/IgG and MDA231i/HMGA1 Ab) were equivalent along time (absolute growth delay of 0 days) and not statistically significant at the end time point ($P = 0.9118$; Fig. 5E, top). Moreover, the incidence of distant metastasis in mice carrying tumors of MDA231i cells pretreated with HMGA1-Ab is significantly reduced in comparison with tumors of MDA231i cells pretreated with an unspecific IgG (P value = 0.0005; Wilcoxon matched-pairs signed rank test; Fig. 5E, bottom, and F; Supplementary Fig. S16). These results suggest that eHMGA1 is involved in the prometastatic effects outlined earlier for HMGA1 (36–38).

The subcellular localization of HMGA1 predicts the incidence of metastasis in TNBC patients

Finally, we evaluated the possible clinical relevance of our *in vitro* and *in vivo* findings in human breast tumor samples. We studied the expression and subcellular localization of HMGA1 in three patient-derived xenograft (PDX) models, representing the three major breast cancer molecular subtypes (luminal-ER$^+$, Her2$^+$, and TNBC). Our findings showed that the luminal model had the lowest expression of HMGA1. In HER2$^+$, the expression was higher than in luminal, but still nuclear. Interestingly, TNBC had the highest expression and clear cytoplasmic localization (Fig. 6A). The results obtained with the PDX models agree with the gene expression analysis obtained from a large TCGA cohort (Supplementary Fig. S1). In order to establish a link between the subcellular localization of HMGA1 in primary human tumors and the incidence of distant metastasis, we assessed HMGA1 expression by IF in 21 primary tumors of TNBC patients who either did or did not develop metastasis and had a minimum follow-up of 6 years from diagnosis (Supplementary Table S1). All (11) primary tumors analyzed of TNBC patients who did not develop metastasis showed a nuclear localization of HMGA1, correlating with a noninvasive phenotype (Fig. 6B; Supplementary Fig. S17). Conversely, all (10) primary tumors analyzed of TNBC patients who developed metastasis presented a cytoplasmic localization of HMGA1, which we previously correlated with HMGA1 secretion (Fig. 6B; Supplementary Fig. S18). Furthermore, normal breast tissue did not have any specific signal for HMGA1 (Fig. 6B; Supplementary Fig. S19). The quantification of HMGA1 expression in TNBC indicates that the cytoplasmic localization of HMGA1 is a promising candidate biomarker at the time of diagnosis that predicts distant metastasis in TNBC patients (Fig. 6C). In TN metastatic breast cancer tumors, there is a shift in the subcellular localization of HMGA1 from the

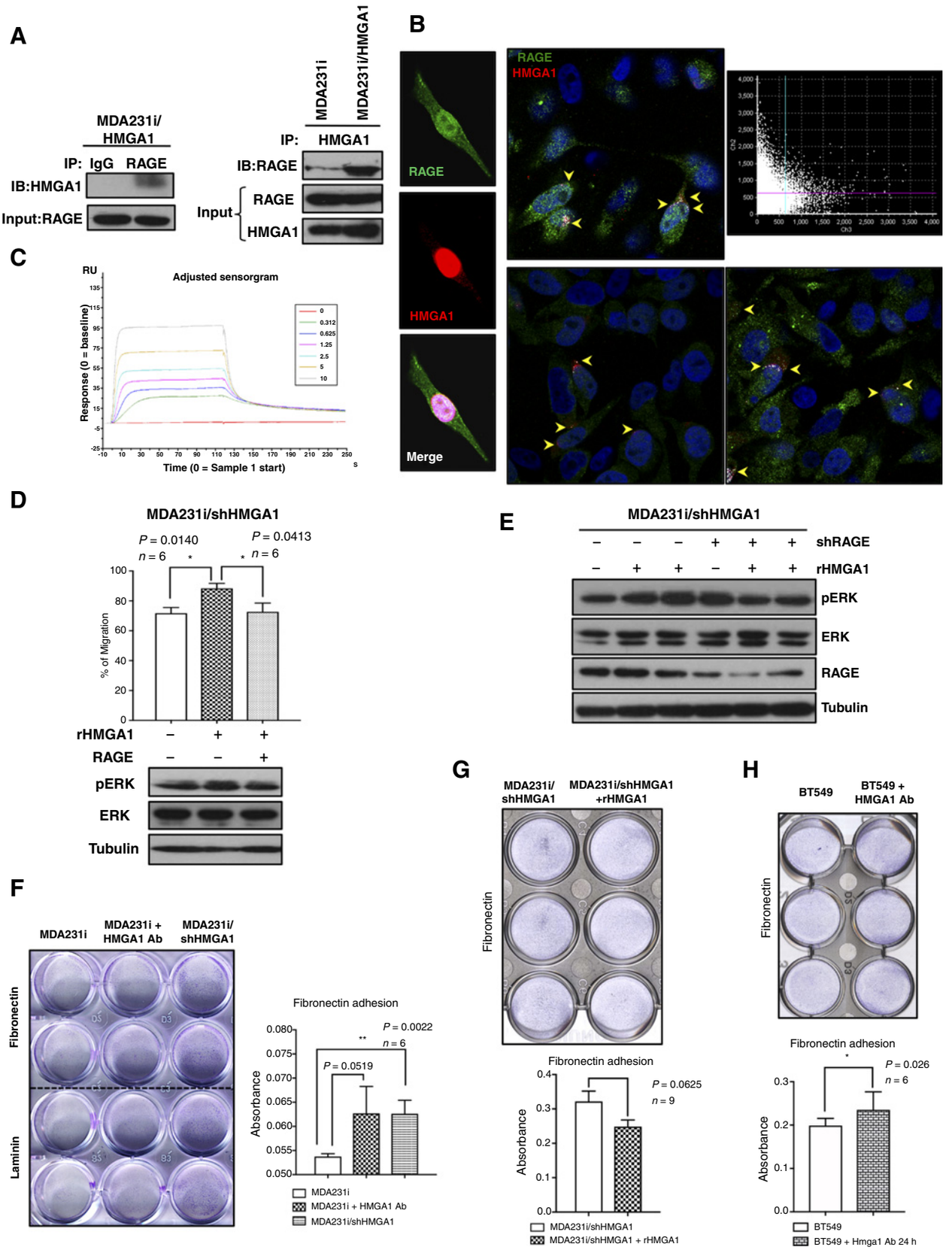

nucleus to the cytoplasm. HMGA1 expression is mostly detected in the cytoplasm (P value < 0.0001). The analysis of the subcellular localization of HMGA1 in TN nonmetastatic tumors shows that their cells have a stronger nuclear expression and lower cytoplasmic expression than in TN metastatic tumors (Fig. 6C). Lastly, we showed that HMGA1 was expressed in different human metastasis which suggests that HMGA1 may play a role not only in tumor invasion but also in establishing distant metastasis (Fig. 6D; Supplementary Fig. S20).

Discussion

There is abundant research showing a correlation between HMGA1 expression and prognosis in cancer (17, 18). In addition, the ectopic overexpression of HMGA1 in tumor cells has been shown to induce a transformed phenotype (39). However, the mechanistic explanation on how HMGA1 exerts its role in tumor progression is not completely established. The current view on HMGA1 oncogenic mechanism is that its ability to modulate chromatin structure and to bind to different transcription factors facilitates the expression of genes involved in tumor progression and metastasis. Recently, the use of gene expression analysis gave rise to different hypothesis on mechanisms used by HMGA1 in tumorigenesis. These studies have suggested the involvement of different signaling pathways such as the Ras/ERK, Wnt/β catenin, Notch, and Hippo signaling pathways in the action of HMGA1 (38, 40–42). However, most of these studies focused on the intracellular role of HMGA1 in cancer. Instead, our research stems from the finding that HMGA1 is secreted in breast tumor–invasive cells and that the extracellular fraction of the protein plays a critical role in the invasive phenotype associated to HMGA1.

Our data show that HMGA1 is overexpressed and secreted in highly invasive TNBC cells. The presence of HMGA1 in the invasive secretome and the lack of signal peptide in its protein sequence imply that HMGA1 cannot follow the classical ER-Golgi pathway for its secretion. Consequently, the levels of eHMGA1 do not change upon the blockage of the ER-Golgi secretory pathway. What we could not anticipate was that HMGA1 does not get secreted through extracellular vesicles. A large fraction of the proteins secreted through unconventional secretion use either exosomes or microvesicles (extracellular vesicles derived from the plasma membrane) for their secretion (12, 13). However, other proteins such as fibroblast growth factor 2 use vesicle-independent nonclassical secretion pathways (43). Our data show that CK2 is involved in the regulation of the secretion of eHMGA1 in invasive breast cancer cells. Based on published data, it is very likely that CK2 phosphorylates HMGA1 in MDA231i cells. There are publications describing the phosphorylation of both, HMGA1 and its close relative HMGA2 by CK2 (32, 44). However, we cannot guarantee that the same happens in our MDA231i cells, since the former studies have been done using different experimental models, including recombinant proteins, prostate and lung cancer cell lines, and human tissues such as placenta (45, 46).

One of the most striking results in this work was that, despite being a theoretically nuclear protein, HMGA1 is secreted and invasive tumor cells treated with blocking Abs against HMGA1 showed a reduction in both migration and invasion. Therefore, just blocking eHMGA1 was enough to prevent the main protumorigenic features linked to HMGA1. Then, our goal was to show the molecular mechanism used by HMGA1 to mediate migration and invasion in the extracellular space. The discovery that pERK activation was modulated by the levels of eHMGA1 or its blockage, together with the finding that treatment with rHMGA1 did not result in the internalization of the protein, led us to think that a membrane receptor could be involved in the cellular signaling induced by eHMGA1. Our quest to find this receptor led to the identification of RAGE. RAGE is a type I transmembrane protein belonging to the immunoglobulin superfamily, involved in the signaling of another nuclear protein from the HMG family (HMGB1; ref. 47), as well as members of the S100 family, the advanced glycation end products (AGEs), and several fibrillar proteins (48, 49). RAGE is generally expressed at very low levels, and its expression has been related to inflammatory and tumorigenic processes. RAGE ligands have in common the presence of motifs containing acidic stretches, and HMGA1 fulfilled this requirement (50). Our data demonstrated that HMGA1 and RAGE interact physically, and that RAGE mediates the activation of pERK induced by eHMGA1. Besides, our data showed that in invasive cells with no intracellular HMGA1, exogenous HMGA1 (rHMGA1) is able to mediate a migratory phenotype

Figure 4.

HMGA1 binds to RAGE inducing pERK signaling and having an impact on cell adhesion. **A** (left plot), MDA231i/HMGA1 cells were used to immunoprecipitate using either an unspecific IgG or RAGE-Ab and probed with HMGA1-Ab. Input represents RAGE expression in total cell lysates. Right plot, WB showing RAGE levels after immunoprecipitate HMGA1-C-6-His-tag using nickel beads. Input represents RAGE and HMGA1 expression in total cell lysates. **B** (left plot), IF of MDA231i cells showing RAGE (green) and HMGA1 (red) expression separately and merged. Right plot, IF of nonpermeabilized MDA231i cells showing RAGE (green) and HMGA1 (red) expression. Hoechst was used to counterstain the nuclei. Pictures are shown with a white mascara, pointed out by yellow arrows to indicate areas of membrane colocalization. Upper right corner of the plot shows the quantification of colocalization of one representative image. **C,** Sensorgrams showing the molecular interaction between HMGA1 and RAGE analyzed by SPR. Overlayed sensorgrams of interaction between immobilized RAGE and different concentrations of rHMGA1 are shown. **D,** Graph showing the percentage of migration of MDA231i/shHMGA1 measured by wound-healing assay. Treatment of the cells with rHMGA1 increased their migration ability, which was abrogated in the presence of recombinant sRAGE. For each condition, WB with pERK and ERK levels is shown. Tubulin was used as loading control. Statistical analysis was done using the Mann–Whitney test. **E,** WB of MDA231i/shHMGA1 and MDA231i/shHMGA1/shRAGE cells treated with rHMGA1. pERK, ERK, and RAGE levels are shown. Tubulin was used as loading control. **F,** Adhesion experiments in MDA231i, MDA231i treated with HMGA1 Ab, and MDA231i/shHMGA1 cells are shown. Left plot, Crystal violet staining of a representative experiment using fibronectin and laminin. Right plot, Graph showing the quantification of adhesion experiments to fibronectin. Reduction of HMGA1 levels increases adhesion to fibronectin. Statistical analysis was done using the Mann–Whitney test. **G,** Adhesion experiments in MDA231i/shHMGA1 treated or not with rHMGA1 are shown. Top panel, Crystal violet staining of a representative experiment using fibronectin. Bottom plot, Graph showing the quantification of adhesion experiments to fibronectin. Treatment of MDA231i/shHMGA1 cells with rHMGA1 reduces adhesion to fibronectin. Statistical analysis was done using the Mann–Whitney test. **H,** Adhesion experiments in BT549 cells are shown. Top plot, Crystal violet staining of a representative experiment using fibronectin. Bottom plot, Graph showing the quantification of adhesion experiments to fibronectin. Treatment with HMGA1 Ab increases the adhesion of BT549 cells to fibronectin. Statistical analysis was done using the Mann–Whitney test.

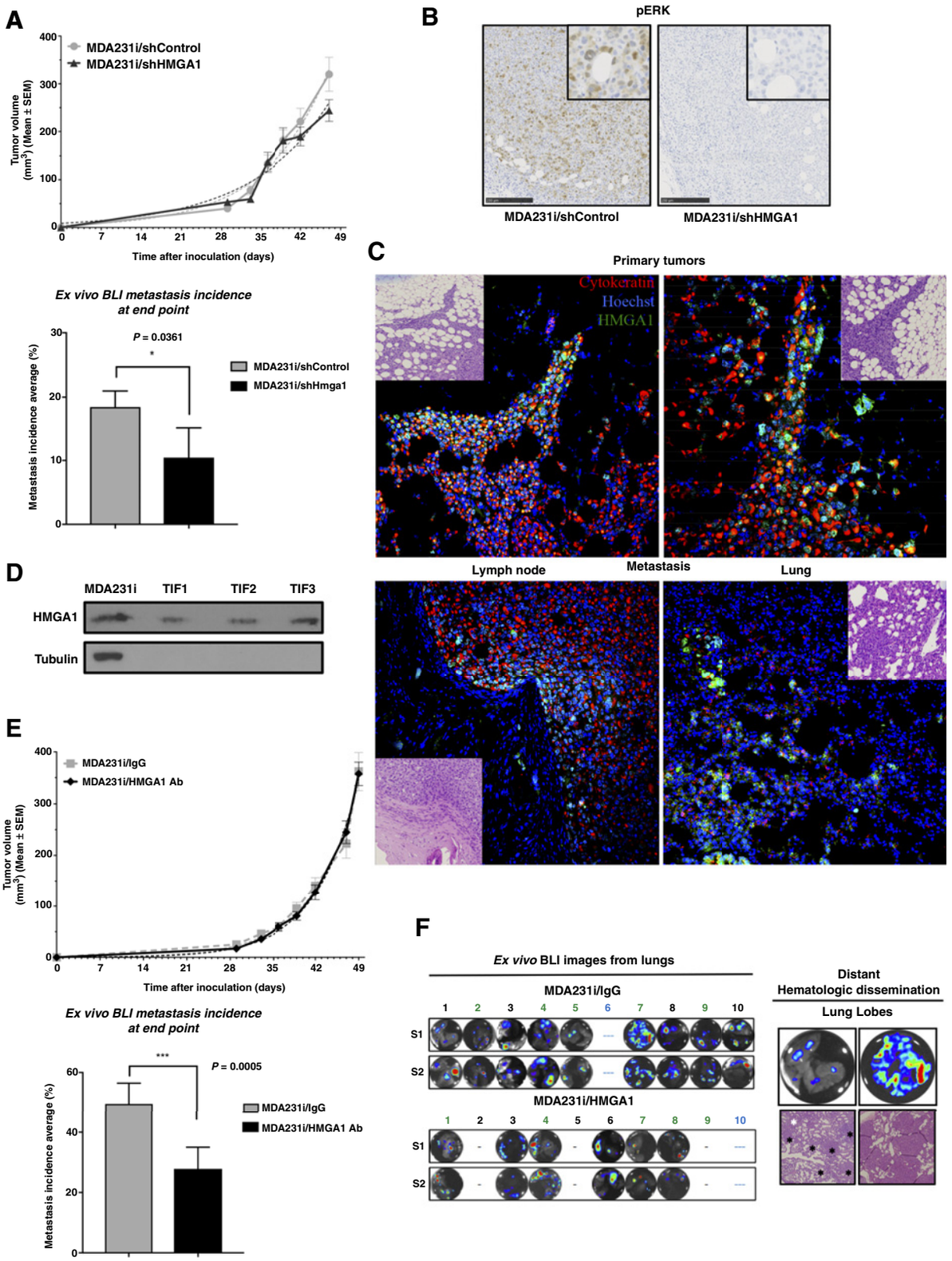

through RAGE. Importantly, these results prove that the proinvasive phenotype induced by eHMGA1 is largely mediated by engaging RAGE signaling.

Besides binding multiple ligands engaging different cellular activities, RAGE's aminoacid sequence shows that it is closely related to genes coding for cell adhesion molecules (47, 50). In fact, RAGE has been found to mediate both cell-to-cell and cell-to-extracellular matrix (ECM) adhesion (51). The ectopic expression of RAGE in tumor cells has been shown to induce an increased adhesion to ECM. Our data show that reduced levels of eHMGA1, due to either knockdown or HMGA1 Ab treatment, induce a higher cell adhesion and a reduction of pERK levels in invasive TNBC cells. In some cases, the binding of a ligand such as S100A7 to RAGE has been linked to tumorigenesis (35). It has also been shown that the binding of HMGB1 to RAGE results in increased levels of ERK1/2 and tumor progression (23). Together, these results show that MDA231i become highly migratory in part because eHMGA1 induces a loss of adhesion upon binding to RAGE. Accordingly, targeting eHMGA1 with a specific Ab increases tumor cell adhesion along with a diminished capacity for migration and invasion.

Furthermore, given the high incidence of metastasis in TNBC, and the previous clinical data linking HMGA1 to tumor aggressiveness and metastasis, we decided to evaluate how the secretion of HMGA1 affects tumorigenesis and whether it has clinical implications for TNBC patients. To do so, we took advantage of the correlation observed both *in vitro* and *in vivo* between a cytoplasmic localization of HMGA1 and its secretion. Our experiments with xenograft models indicate first that HMGA1 expression is enriched both in the invasive front of primary tumors and in metastatic *foci*. The results also showed that the total cellular levels of HMGA1 correlate with the incidence of metastasis, but do not affect significantly primary tumor growth. We also proved that the lower incidence of metastasis caused by stable ablation of HMGA1 expression correlates with a decrease in pERK expression in the primary tumor, confirming our *in vitro* data. Our *in vivo* results do not fully agree with other published reports on HMGA1. Although most studies report a correlation between HMGA1 levels and the incidence of invasion and metastasis, most of them also show a correlation with tumor cell proliferation (36). However, our data indicate that HMGA1 levels do not correlate with tumor growth, in concordance with our *in vitro* data that show no significant effect of HMGA1 expression in cell proliferation. There is one report done with MDA-MB-231 cells where the authors describe a proliferation phenotype linked to HMGA1 that we do not see, although we both observe a metastatic phenotype (36). We believe that the discrepancy could be due to MDA-MB-231 is a highly heterogeneous cell line.

In this work, we wanted to evaluate the specific implication of the extracellular fraction of HMGA1 in the setting of tumor invasion and metastasis in TNBC. Taking into consideration our *in vitro* data that prove that an Ab against HMGA1 is able to increase adhesion and block the migration an invasion mediated by eHMGA1, we tested the effect of pretreating cells with HMGA1-Ab before implanting them in immunodeficient mice. Our data showed a clear decrease in the incidence of metastasis, highlighting the importance of eHMGA1 in the metastatic process. Then, to correlate our *in vitro* and *in vivo* results with patient samples, we used the observation that an oversecretion of HMGA1 implies a visible change in HMGA1 subcellular localization in tumor cells and tissue. Our experiments with xenograft models showed a clear correlation between a cytoplasmic localization of HMGA1 and its secretion measured in the TIF isolated from primary tumors. Therefore, we used the cytoplasmic localization of HMGA1 as a surrogate of its secretion in human tumor tissue sections. This observation was used to measure HMGA1 retrospectively in a series of 21 TNBC primary tumors with enough follow-up to know whether they did or did not develop distant metastasis. The results show that the subcellular localization of HMGA1 predicts the incidence of metastasis at the primary tumor stage in TNBC, correlating the cytoplasmic expression of HMGA1 with the metastatic phenotype. Furthermore, the expression of HMGA1 in different human metastasis emphasizes the possible role of HMGA1 in the establishment and maintenance of distant metastasis.

In summary, we have proved that HMGA1 is oversecreted in a regulated fashion in TNBC-invasive cells. Once in the extracellular space, HMGA1 becomes a ligand for RAGE. Upon HMGA1 binding, RAGE signals through pERK, increasing migration and invasion in invasive TNBC cells. Besides, the ablation of HMGA1 and the blockage of eHMGA1 cause an increase in cellular adhesion. We have also demonstrated that blocking the extracellular function of HMGA1 using blocking Abs blocks both the promigratory and the proinvasive phenotypes caused by HMGA1 (Fig. 7). We believe the findings

Figure 5.

Role of HMGA1 in the tumorigenic and metastatic ability on an orthotopic breast cancer model. **A,** (top plot) Tumor growth rates of MDA231i/shControl (●) and MDA231i/shHMGA1 (▲) cells from time of implantation to experimental end point. Tumor growth was monitored by conventional caliper measurement. Growth rates comparative statistics was done using a nonparametric Mann–Whitney *U* test. Bottom plot, Incidence of spontaneous metastatic dissemination patterns of MDA231i/shControl (gray bars) and MDA231i/shHMGA1 (black bars) tumors. The presence of metastasis was identified by *ex vivo* BLI. **B,** pERK immunohistochemistry from a representative MDA231i/shControl and MDA231i/shHMGA1 tumors is shown. **C,** IF of representative tumors (top plot) and metastasis (bottom plot) derived from MDA231i cells. HMGA1 expression (green) increased toward the invasive front (top plot), and it is also founded in metastatic *foci*. Cytokeratin (red) is used to stain human epithelial cells, and Hoechst to counterstain the nuclei. Representative confocal images are shown with the corresponding H&E images. **D,** WB showing HMGA1 expression levels in MDA231i cells and in TIFs obtained from 3 different tumors derived from MDA231i cells. Tubulin was used as loading control and to check absence of whole lysates in TIFs' samples. **E,** (top plot) Tumor growth rates of MDA231i cells pretreated either with an unspecific IgG (■) or with HMGA1-Ab (◆) from time of implantation to experimental end point. Bottom plot, Incidence of spontaneous metastatic dissemination patterns of MDA231i pretreated either with an unspecific IgG (gray bars) or with HMGA1-Ab (black bars). **F,** Representative *ex vivo* BLI images. Left plot, *Ex vivo* BLI images from lungs of MDA231i/IgG and MDA231i/IgG-bearing mice. Right plot, Examples of *ex vivo* images and histopathology of a representative distant hematologic dissemination into lungs (isolated micrometastases in the interstitium of the lung and tumoral embolus occluding peribronchial blood vessels). Black asterisks indicate tumor cells, and white asterisks indicate normal tissue. When nothing is indicated, the H&E is all tumor.

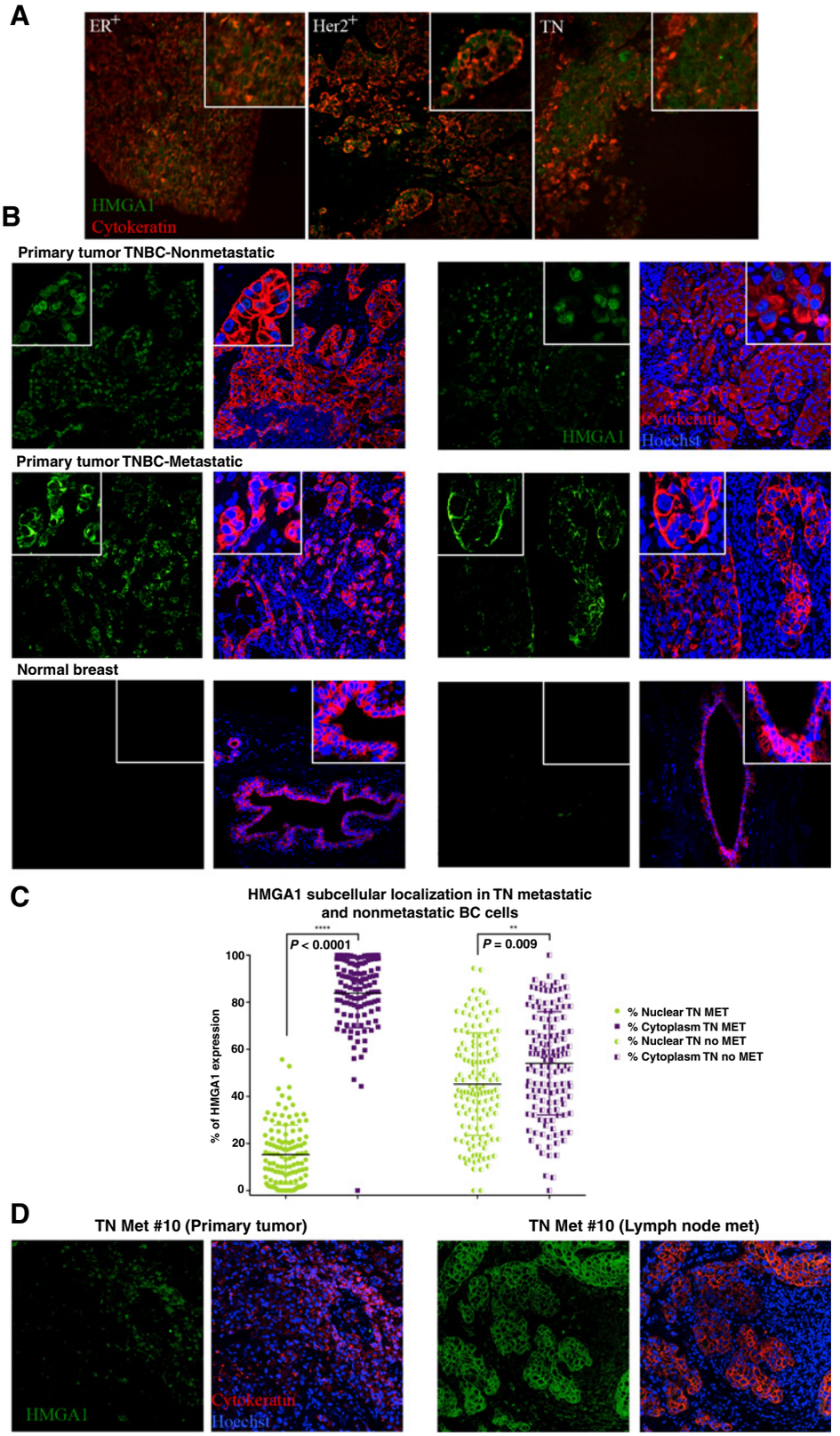

Figure 6.

HMGA1 expression and subcellular localization in human breast cancer samples. **A,** IF of 3 PDXs representing the major subtypes of breast cancer: ER^+, $HER2^+$, and TNBC. HMGA1 expression is shown in green. Cytokeratin (red) is used to stain human epithelial cells. Representative confocal images are shown. **B,** IF of human primary tumors from patients with TNBC, both nonmetastatic and metastatic, as well as normal breast tissue. Two representative samples from each group are shown. For each sample, HMGA1 expression (green) is shown separately. Next to them, the same image is showing cytokeratin expression (red) and Hoechst. The top corner shows a higher magnification of each image. **C,** Graph representing the measurements of HMGA1 expression in the nuclei and in the cytoplasm of four representative TNBC primary tumors from patients who develop distant metastasis (TN Met) and four that did not (TN no Met). Thirty cells from a representative field of each sample were randomly selected for measurements. Image J software was used for the analysis. The Wilcoxon matched-pairs signed rank test was used to compared nuclear and cytoplasmic HMGA1 expression. **D,** IF of human metastasis from patients with TNBC. Two representative samples are shown. HMGA1 expression (green) is shown separately, and next to them, the same image is showing cytokeratin expression (red) and Hoechst.

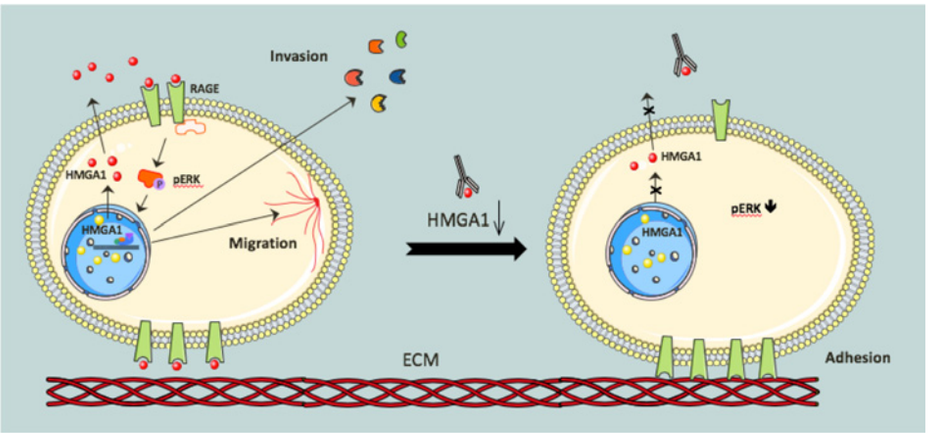

Figure 7.
eHMGA1 mechanism of action.

described in this work are especially relevant due to the increasing interest in identifying new biomarkers and drug targets for TNBC. In addition, we believe these results conceptually change the view on HMGA1's role in tumorigenesis. Finally, our results highlight the potential relevance of unconventional protein secretion in cancer diagnostics and therapeutics, particularly in tumor types that do not appear to be primarily driven by gene mutations.

Disclosure of Potential Conflicts of Interest

No potential conflicts of interest were disclosed.

Authors' Contributions

Conception and design: O. Méndez, J. Pérez, J. Tabernero, J. Villanueva
Development of methodology: O. Méndez, C. Salvans, M. Pujals, Y. Fernández, I. Abasolo, S. Schwartz Jr, J. Villanueva
Acquisition of data (provided animals, acquired and managed patients, provided facilities, etc.): O. Méndez, V. Peg, I. Abasolo, J. Pérez, A. Matres, M. Valeri, L. Villarreal, S. Schwartz Jr, S. Ramon y Cajal, J. Tabernero, J. Cortés, J. Arribas
Analysis and interpretation of data (e.g., statistical analysis, biostatistics, computational analysis): O. Méndez, V. Peg, Y. Fernández, I. Abasolo, J. Pérez, M. Valeri, J. Gregori, S. Schwartz Jr, J. Tabernero, J. Villanueva
Writing, review, and/or revision of the manuscript: O. Méndez, Y. Fernández, I. Abasolo, J. Pérez, S. Schwartz Jr, S. Ramon y Cajal, J. Tabernero, J. Cortés, J. Arribas, J. Villanueva
Administrative, technical, or material support (i.e., reporting or organizing data, constructing databases): J. Tabernero
Study supervision: J. Villanueva

Acknowledgments

We thank Dr. Laia Foradada and Natalia García-Aranda from FVPR for their assistance in the *in vivo* studies. We also thank Dr. Beatriz Morancho for her assistance in the obtention of PDX tumor samples. We thank Dr. Paolo Nuciforo from the Molecular Pathology Core lab for assistance in tumor tissue processing procedures. We thank Drs. Elena García-Fruitós, Paolo Saccardo, and Antonio Villaverde from the Protein Production Platform of CIBER in Bioengineering, Biomaterials & Nanomedicine (CIBER-BBN)/IBB, at the UAB for their assistance in the recombinant production of HMGA1. We thank Dr. Silvia Barceló from Idibell for her help in the SPR analysis. We thank Dr. Alex Sánchez Pla from the statistics and bioinformatics unit of VHIR, for his advice in the statistical analysis of the article. This work was supported by grants from Instituto Salud Carlos III (FIS PI15/00357) and cofunded by FEDER, the FERO and Josep Botet Foundations. J. Villanueva was supported by the Miguel Servet Program, Instituto Salud Carlos III, and cofunded by FEDER and by the Susan G. Komen Foundation (CCR15333737). O. Méndez was supported by a Peris grant (Generalitat de Catalunya, Departament de salut). J. Arribas is funded by the Breast Cancer Research Foundation (BCRF, grant BCRF-17-008) and Instituto de Salud Carlos III (PI16/00253). Y. Fernández, S. Schwartz Jr, and I. Abasolo acknowledge grants from CIBER-BBN (PENTRI Intramural Grant), "Fundació Marató TV3" (PENTRI project 337/C/2013), and SGR (2014 SGR 1394).

The costs of publication of this article were defrayed in part by the payment of page charges. This article must therefore be hereby marked *advertisement* in accordance with 18 U.S.C. Section 1734 solely to indicate this fact.

Received February 19, 2018; revised June 14, 2018; accepted August 13, 2018; published first August 22, 2018.

References

1. Hudis CA, Gianni L. Triple-negative breast cancer: an unmet medical need. Oncologist 2011;16:1–11.
2. Shastry M, Yardley DA. Updates in the treatment of basal/triple-negative breast cancer. Curr Opin Obstet Gynecol 2013;25:40–8.
3. Chaffer CL, Weinberg RA. A perspective on cancer cell metastasis. J Cell Sci 2011;331:1–6.
4. Schaaij-Visser TBM, de Wit M, Lam SW, Jiménez CR. The cancer secretome, current status and opportunities in the lung, breast and colorectal cancer context. Biochim Biophys Acta 2013;1834:2242–58.
5. Paltridge JL, Belle L, Khew-Goodall Y. The secretome in cancer progression. Biochim Biophys Acta 2013;1834:2233–41.
6. Méndez O, Villanueva J. Challenges and opportunities for cell line secretomes in cancer proteomics. Prot Clin Appl 2015;9:348–57.
7. Villarreal L, Méndez O, Salvans C, Gregori J, Baselga J, Villanueva J. Unconventional secretion is a major contributor of cancer cell line secretomes. Mol Cell Proteomics 2013;12:1046–60.
8. Katsila T, Juliachs M, Gregori J, Macarulla T, Villarreal L, Bardelli A, et al. Circulating pEGFR is a candidate response biomarker of cetuximab therapy in colorectal cancer. Clin Cancer Res 2014;20:6346–56.
9. Butler GS, Overall CM. Proteomic identification of multitasking proteins in unexpected locations complicates drug targeting. Nat Rev Drug Discov 2009;8:935–48.
10. Eustace BK, Sakurai T, Stewart JK, Yimlamai D, Unger C, Zehetmeier C, et al. Functional proteomic screens reveal an essential extracellular role for hsp90α in cancer cell invasiveness. Nat Cell Biol 2004;6:507–14.

11. Rovere-Querini P, Capobianco A, Scaffidi P, Valentinis B, Catalanotti F, Giazzon M, et al. HMGB1 is an endogenous immune adjuvant released by necrotic cells. EMBO Rep 2004;5:825–30.
12. Rabouille C, Malhotra V, Nickel W. Diversity in unconventional protein secretion. J Cell Sci 2012;125:5251–5.
13. Nickel W, Rabouille C. Mechanisms of regulated unconventional protein secretion. Nat Rev Mol Cell Biol 2009;10:148–55.
14. Shah SN, Resar LMS. High mobility group A1 and cancer: potential biomarker and therapeutic target. Histol Histopathol 2012;27:567–79.
15. Cleynen I, Huysmans C, Sasazuki T, Shirasawa S, Van de Ven W, Peeters K. Transcriptional control of the human high mobility group A1 gene: basal and oncogenic Ras-regulated expression. Cancer Res 2007;67:4620–9.
16. Fusco A, Fedele M. Roles of HMGA proteins in cancer. Nat Rev Cancer 2007;7:899–910.
17. Piscuoglio S, Zlobec I, Pallante P, Sepe R, Esposito F, Zimmermann A, et al. HMGA1 and HMGA2 protein expression correlates with advanced tumour grade and lymph node metastasis in pancreatic adenocarcinoma. Histopathology 2012;60:397–404.
18. Hristov AC, Cope L, Di Cello F, Reyes MD, Singh M, Hillion JA, et al. HMGA1 correlates with advanced tumor grade and decreased survival in pancreatic ductal adenocarcinoma. Mod Pathol 2009;23:98–104.
19. Méndez O, Zavadil J, Esencay M, Lukyanov Y, Santovasi D, Wang S-C, et al. Knock down of HIF-1α in glioma cells reduces migration in vitro and invasion in vivo and impairs their ability to form tumor spheres. Mol Cancer 2010;9:133.
20. Gregori J, Villarreal L, Méndez O, Sánchez A, Baselga J, Villanueva J. Batch effects correction improves the sensitivity of significance tests in spectral counting-based comparative discovery proteomics. J Proteomics 2012; 75:3938–51.
21. Abe A, Kuwata T, Yamauchi C, Higuchi Y, Ochiai A. High Mobility Group Box1 (HMGB1) released from cancer cells induces the expression of pro-inflammatory cytokines in peritoneal fibroblasts. Pathol Int 2014;64:267–75.
22. Gardella S, Andrei C, Ferrera D, Lotti LV, Torrisi MR, Bianchi ME, et al. The nuclear protein HMGB1 is secreted by monocytes via a non-classical, vesicle-mediated secretory pathway. EMBO Rep 2002;3:995–1001.
23. Nehil M, Paquette J, Tokuyasu T, McCormick F. High mobility group box 1 promotes tumor cell migration through epigenetic silencing of semaphorin 3A. Oncogene 2013;33:5151–62.
24. Peluso S, Chiappetta G. High-Mobility Group A (HMGA) proteins and breast cancer. Breast Care 2010;5:81–5.
25. Di Cello F, Shin J, Harbom K, Brayton C. Knockdown of HMGA1 inhibits human breast cancer cell growth and metastasis in immunodeficient mice. Biochem Biophys Res Commun 2013;1–18.
26. Liau SS, Rocha F, Matros E, Redston M, Whang E. High mobility group AThook 1 (HMGA1) is an independent prognostic factor and novel therapeutic target in pancreatic adenocarcinoma. Cancer 2008;113: 302–14.
27. Frasca F, Rustighi A, Malaguarnera R, Altamura S, Vigneri P, Del Sal G, et al. HMGA1 inhibits the function of p53 family members in thyroid cancer cells. Cancer Res 2006;66:2980–9.
28. Koboldt DC, Fulton RS, McLellan MD, Schmidt H, Kalicki-Veizer J, McMichael JF, et al. Comprehensive molecular portraits of human breast tumours. Nature 2012;490:61–70.
29. Kho DH, Zhang T, Balan V, Wang Y, Ha SW, Xie Y, et al. Autocrine motility factor modulates EGF-mediated invasion signaling. Cancer Res 2014;74: 2229–37.
30. de Abreu da Silva IC, Carneiro VC, de Moraes Maciel R, da Costa RFM, Furtado DR, Bastos de Oliveira FM, et al. CK2 phosphorylation of schistosoma mansoni HMGB1 protein regulates its cellular traffic and secretion but not its DNA transactions. PLoS One 2011;6:e23572.
31. Mor-Vaknin N, Punturieri A, Sitwala K, Faulkner N, Legendre M, Khodadoust MS, et al. The DEK nuclear autoantigen is a secreted chemotactic factor. Mol Cell Biol 2006;26:9484–96.
32. Sgarra R, Maurizio E, Zammitti S, Sardo Lo A, Giancotti V, Manfioletti G. Macroscopic differences in HMGA oncoproteins post-translational modifications: C-terminal phosphorylation of HMGA2 affects its DNA binding properties. J Proteome Res 2009;8:2978–89.
33. Zhao C-B, Bao J-M, Lu Y-J, Zhao T, Zhou X-H, Zheng D-Y, et al. Co-expression of RAGE and HMGB1 is associated with cancer progression and poor patient outcome of prostate cancer. Am J Cancer Res 2014; 4:369–77.
34. Schmidt AM, Yan SD, Yan SF, Stern DM. The multiligand receptor RAGE as a progression factor amplifying immune and inflammatory responses. J Clin Invest 2001;108:949–55.
35. Nasser MW, Wani NA, Ahirwar DK, Powell CA, Ravi J, Elbaz M, et al. RAGE mediates S100A7-induced breast cancer growth and metastasis by modulating the tumor microenvironment. Cancer Res 2015;75:974–85.
36. Shah SN, Cope L, Poh W, Belton A, Roy S, Talbot CC, et al. HMGA1: a master regulator of tumor progression in triple-negative breast cancer cells. PLoS One 2013;8:e63419.
37. Wang EL, Qian ZR, Rahman MM, Yoshimoto K, Yamada S, Kudo E, et al. Increased expression of HMGA1 correlates with tumour invasiveness and proliferation in human pituitary adenomas. Histopathology 2010; 56:501–9.
38. Pegoraro S, Ros G, Piazza S, Sommaggio R, Ciani Y, Rosato A, et al. HMGA1 promotes metastatic processes in basal-like breast cancer regulating EMT and stemness. Oncotarget 2013;4:1293–308.
39. Reeves R, Edberg DD, Li Y. Architectural transcription factor HMGI(Y) promotes tumor progression and mesenchymal transition of human epithelial cells. Mol Cell Biol 2001;21:575–94.
40. Resmini G, Rizzo S, Franchin C, Zanin R, Penzo C, Pegoraro S, et al. HMGA1 regulates the Plasminogen activation system in the secretome of breast cancer cells. Sci Rep 2017;7:11768.
41. Treff NR, Pouchnik D, Dement GA, Britt RL, Reeves R. High-mobility group A1a protein regulates Ras/ERK signaling in MCF-7 human breast cancer cells. Oncogene 2004;23:777–85.
42. Pegoraro S, Ros G, Ciani Y, Sgarra R, Piazza S, Manfioletti G. A novel HMGA1-CCNE2-YAP axis regulates breast cancer aggressiveness. Oncotarget 2015;6:19087–101.
43. Nickel W. The unconventional secretory machinery of fibroblast growth factor 2. Traffic 2011;12:799–805.
44. Palvino J, Linnala-Kankkunen A. Identification of sites on chromosomal protein HMG-I phosphorylated by casein II. FEBS Lett 2001;257:101–4.
45. Jiang X, Wang Y. Acetylation and phosphorylation of high-mobility group A1 proteins in PC-3 human tumor cells. Biochemistry 2006; 45:7194–201.
46. Ferranti P, Malorni A, Marino G, Pucci P, Goodwin GH, Manfioletti G, et al. Mass spectrometric analysis of the HMGY protein from lewis lung carcinoma. Identification of phosphorilation sites. J Biol Chem 2018;267: 22486–9.
47. Hori O, Brett J, Slattery T, Cao R, Zhang J, Chen JX, et al. The receptor for advanced glycation end products (RAGE) is a cellular binding site for amphoterin. Mediation of neurite outgrowth and co-expression of rage and amphoterin in the developing nervous system. J Biol Chem 1995;270: 25752–61.
48. Arumugam T, Simeone DM, Schmidt AM, Logsdon CD. S100P stimulates cell proliferation and survival via receptor for activated glycation end products (RAGE). J Biol Chem 2004;279:5059–65.
49. Xie J, Méndez JD, Méndez-Valenzuela V, Aguilar-Hernández MM. Cellular signalling of the receptor for advanced glycation end products (RAGE). Cell Signal 2013;25:2185–97.
50. Fritz G. RAGE: a single receptor fits multiple ligands. Trends Biochem Sci 2011;36:625–32.
51. Sessa L, Gatti E, Zeni F, Antonelli A, Catucci A, Koch M, et al. The receptor for advanced glycation end-products (RAGE) is only present in mammals, and belongs to a family of Cell Adhesion Molecules (CAMs). PLoS One 2014;9:e86903–13.